Journal of Sound and Vibration (2000) **232**(1), 193–211
doi:10.1006/jsvi.1999.2693, available online at http://www.idealibrary.com on IDEAL®

MEASUREMENT OF NEW ENERGETIC PARAMETERS FOR THE OBJECTIVE CHARACTERIZATION OF AN OPERA HOUSE

D. STANZIAL AND D. BONSI

CIARM-CNR c/o Cemoter, v. Canal Bianco, 28-44044 Cassana, Ferrara, Italy

AND

N. PRODI

CIARM c/o Dipartimento di Ingegneria, Università di Ferrara, v. Saragat, I-44100 Ferrara, Italy

(*Accepted* 30 *June* 1999)

Following a rigorous approach to the energetic analysis of sound fields, the measurement of new quantities for the physical description of the behavior of sound in enclosed spaces has been carried out inside an Italian opera house. A first set of measures has been performed during the steady state, allowing the study of the new discovered property called *sound intensity polarization*, which accounts for the amount of energy oscillating thorugh the measurement point. Then, in order to accomplish a complete statistical study of the transient field behaviour, the full set of quantities involved in the energy continuity equation (total sound energy density and intensity) has been obtained by means of the extension of the classical Schroeder's method to the quantities depending also on the air particle velocity solution of the wave equation. Finally, two newly defined field indicators, accounting for the local amount of sound energy radiation and the balance between the potential and kinetic parts of the total sound energy density, have been investigated.

1. INTRODUCTION

A new theoretical approach to the energetic analysis of general sound fields has been developed and validated in recent years [1]. Following this approach, which rigorously accounts for the wave nature of the sound field, a physically meaningful bipartition of the instantaneous sound intensity has been introduced [2] and the two defined quantities have been interpreted as the *radiating* and *oscillating* components of the sound intensity [3]. This interpretation is consistent with their respective time-average values: always vanishing for the oscillating component but usually different from zero for the radiating one. The time-average radiating intensity coincides with the well-known definition of the active intensity vector quantity [4], while the term *sound intensity polarization* has been inaugurated for

0022-460X/00/160193 + 19 $35.00/0

the time-averaged oscillating intensity which is a second order symmetric tensor accounting for the oscillations of sound energy in the three-dimensional physical space. Thus, the term *polarization* used in this context is not referred to as a characteristic of the sound propagation (which of course cannot be "polarized" due to the longitudinal nature of the sound wave) but as a spatial property of the time-averaged oscillating intensity. Now, this kind of intensimetric analysis is essentially a time-stationary one and so it can be usefully employed when the steady state conditions of the sound field have to be investigated. However, when the transient field—as for instance the one generated during a usual musical performance—is also of special interest, the standard statistical analysis based on the sound pressure impulse response is of course the more appropriate. As known, the time-stationary and transient behaviours of the sound field are linked to each other through the ergodicity of the acoustic system. This fact determined in the 1960s the major innovation in the room acoustics methods for determining the reverberation time. In fact, as implicitly assumed by Schroeder, the time-stationary average over a continuous random sound pressure signal and the ensemble average over its sampled transients calculated at the initial instant of the decay coincide. Thus, some information regarding the steady state of the acoustic system can be grasped from the transient analysis and *vice versa.* Unfortunately, from a rigorous energetic viewpoint, the standard analysis lacks information regarding the transient behavior of the air particle velocity and so an extension of the well-known Schroeder's method [5], in order to obtain the air particle velocity impulse response corresponding to the same pressure stimulus, is needed. This task has been accomplished in reference [6] and will be briefly summarized below.

This paper accounts for the first measurement campaign performed inside an Italian opera house following the above-mentioned energetic full analysis of the sound field, with the aim of illustrating the new developed techniques, the methods and their potentiality in the field of architectural acoustics. Sections 2 and 3 respectively report the collected experimental data for the steady *sound intensity polarization* and the complete energetic analysis of the transient field performed on the basis of the appropriate extension of the Schroeder's method. The following subsections are devoted to the operative definition of the measured quantities and to the description of experimental set-up used in the opera house.

1.1. THE SOUND INTENSITY POLARIZATION

For the scopes of the present paper it suffices to recall the definition of *oscillating intensity* whose physical interpretation is given in reference [3],

$$\mathbf{r}(t) = \mathbf{j}(t) - \mathbf{a}(t) = p\mathbf{v} - \frac{p^2\langle p\mathbf{v}\rangle}{\langle p^2\rangle} \tag{1}$$

where $\mathbf{j} = \mathrm{p}\mathbf{v}$ is the usual instantaneous sound intensity,

$$\mathbf{a}(t) = \frac{p^2\langle p\mathbf{v}\rangle}{\langle p^2\rangle} \tag{2}$$

is the *radiating intensity*, p and $\mathbf{v}$ are the sound pressure and the particle velocity respectively while $\langle\cdot\rangle$ stands for the stationary time-average process. It is easily shown that the usual active intensity $\mathbf{I}$ coincides with the time-average radiating intensity $\mathbf{A}$ since the following chain of identities holds:

$$\mathbf{I} = \langle \mathbf{j} \rangle = \langle p\mathbf{v} \rangle = \left\langle \frac{p^2 \langle p\mathbf{v} \rangle}{\langle p^2 \rangle} \right\rangle = \langle \mathbf{a} \rangle = \mathbf{A}.$$

On the other hand, since $\langle \mathbf{r} \rangle = \mathbf{0}$ by definition, the second order statistical moment

$$\mathfrak{R} = \sqrt{2\langle \mathbf{r} \otimes \mathbf{r} \rangle} \tag{3}$$

must be evaluated to get a suitable measure of oscillations of energy. Roughly speaking, both the magnitudes of $\mathbf{A}$ and $\mathfrak{R}$ can be evaluated respectively as

$$|\mathbf{A}| = \sqrt{\sum_i A_i^2}, \quad R := \|\mathfrak{R}\| = \sqrt{\sum_{i=j} \mathfrak{R}_{ij}^2}, \qquad i,j = 1,2,3, \tag{4}$$

and converted to a dB *re* $10^{-12}\,\mathrm{W/m^2}$ scale so obtaining a handling definition for the levels of the two different kinds of sound intensities. These two intensity levels can be respectively indicated as L_I and L_R. A more detailed representation of the tensor field $\mathfrak{R}$ is achieved by plotting its characteristic ellipsoid (indicatrix quadric) [2] in the intensity space, so obtaining all possible information regarding the oscillations of sound energy in the three-dimensional physical space. In fact, the eigenvectors of $\mathfrak{R}$ define the spatial orientation of the intensity ellipsoid in the ordinary space where the sound field is defined. Precisely, this latter kind of representation of $\mathfrak{R}$ is visualized in the section 2 for three locations inside the "Teatro Comunale" in Ferrara.

The measurement of the sound intensity polarization has been accomplished by means of a dedicated sound intensity-meter entirely developed using the virtual instrument facility of the *LabView*® system.

1.2. THE EXTENSION OF SCHROEDER'S METHOD

The well-known formula

$$\overline{p^2(t)} = \int_t^\infty [g_p(t')]^2 \, \mathrm{d}t', \tag{5}$$

due to Schroeder [5], is obtained expressing the pressure signal p at the receiving point as a time convolution between a white-noise source term and the pressure impulse response $g_p(t)$, and then calculating the ensemble average (denoted by the upper bar) of the quantity p^2 at any fixed time t. The identity of equation (5) follows due to the autocovariance properties of the stationary white noise. In quite a similar way it can be shown that—in correspondence to the same physical source term leading to equation (5)—the following relation holds for any component of the air particle velocity:

$$\overline{v^2(t)} = \int_t^\infty [g_v(t')]^2 \, \mathrm{d}t', \tag{6}$$

Here $g_v(t)$ is the corresponding component of the air particle velocity impulse response linked to $g_p(t)$ via the Euler equation as detailed in Appendix A.

By combining now equations (5) and (6), following the definitions of the sound energy density $w(t)$ and of any component of the sound intensity $j(t) = p(t)v(t)$, the expressions for the statistical average of the two quantities are readily obtained:

$$\overline{w(t)} = \frac{1}{2}\rho_0 \int_t^\infty \left\{ \frac{[g_p(t')]^2}{z^2} + [g_v(t')]^2 \right\} \mathrm{d}t', \quad \overline{j(t)} = \int_t^\infty [g_p(t')g_v(t')]\,\mathrm{d}t'. \qquad (7, 8)$$

Thus equations (7) and (8) allow one to perform a complete statistical energetic analysis of the transient field behavior and constitute the rigourous extension of the standard Schroeder's method usually employed for evaluating the reverberation time upon considering only the sound potential energy density decay. Precisely, these two expressions will be employed in section 3 for our full energetic analysis. Here we simply note that while the decay curves plotted for the energy densities are always monotonic decreasing functions of time, according to the differential property $\partial\overline{w(t)}/\partial t \leqslant 0$, the same is not true for any component of the sound intensity expressed by equation (8), showing in general an oscillatory behavior between negative and positive values.

1.3. NEW ENERGETIC FIELD INDICATORS: THE ENERGY PARTITION AND THE RADIATIVE TRANSFER

As regards the stationary time-average parts of the global sound energy density—i.e., the averaged potential and kinetic sound energy densities—the following field indicator has been introduced [2]:

$$\sigma = \frac{2\sqrt{W_{Pot}W_{Kin}}}{W_{Pot} + W_{Kin}}. \qquad (9)$$

This indicator, where $W_{Pot} = \frac{1}{2}\rho_0\langle p^2\rangle/z^2$ and $W_{Kin} = \frac{1}{2}\rho_0 v^2$ stand respectively for the time-averaged potential and kinetic sound energy densities, ρ_0 is the air density when no sound is present and z is the characteristic impedance of the air, represents the balance between W_{Pot} and W_{Kin} in the total sound energy density $W = W_{pot} + W_{kin}$. It is easily seen that σ is equal to 1 when an exact balance between W_{pot} and W_{kin} exists at a certain location of the sound field while it is 0 when one of the two parts is equal to zero (for instance at the pressure or velocity nodes of a standing wave). In general sound fields this indicator has intermediate values: $0 < \sigma < 1$.

Another useful indicator introduced and indicated by η in reference [2] on the basis of the velocity of energy transferred by the active intensity defined in reference [1] has the expression

$$\eta = |\mathbf{A}|/cW \qquad (10)$$

and represents the fraction ($0 \leqslant \eta \leqslant 1$) of mean energy which is radiated from any location in the sound fields at the speed of sound c. This interpretation is the

extension to general fields of an argument originally stated by Morse for monopole sound radiation fields (see reference [7]).

Both the values of the indicators defined in equations (9) and (10) have been measured at different locations inside an Italian opera house and will be reported below.

1.4. THE EXPERIMENTAL SET-UP IN THE OPERA HOUSE

Figure 1 shows, on the left side, a plan of the opera house sketching the measurement reference frames at the three tested locations. The points at the mouth of the first order boxes no. 17 and 7 are about 3 m over the wooden floor of the hall, while the point at the central stall along the 11th row of upholstered seats was at about 1·4 m from the floor. The stage of the opera house was prepared with the wooden orchestra shell and the hall was empty. A dodecaedric source was placed in the middle of the stage at about 1·5 m above the floor and feeded with an MLS signal. On the right side of the same figure a sketch of the employed measurement chain is shown. The steady state measurements were taken by using the on purpose developed sound intensity meter (called eNeRGy meter) capable of measuring the new defined intensimetric quantities. The instrument, owing to the simultaneous acquisition of the six channels coming from a 3-D sound intensity probe B&K 4181 provided with a 5 cm spacer) is capable of measuring at once the sound pressure, the air particle velocity, the active intensity and the sound intensity polarization. The last quantity in particular involves the measurement of the six independent components of the second order tensor of equation (3) which, as said above, can be geometrically represented as an ellipsoid in the intensity space. The transient

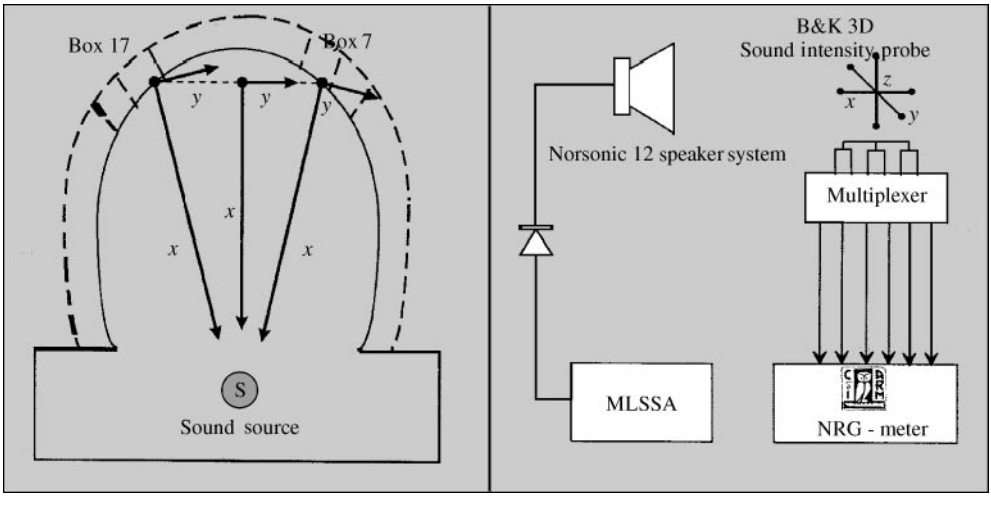

Figure 1. Experimental set-up in the opera house. Left: the reference frame of the three measurement points (the z-axis is normal to the plan and directed towards the ceiling). Right: sketch of the measurment chain. NRG-meter is the virtual instrument specifically developed for measuring the new defined intensimetric quantities.

measurements were carried out by means of a commercial MLS system acquiring the six probe channels sequentially.

2. STEADY STATE INTENSIMETRIC MEASUREMENTS

With the aim of illustrating the basic features and physical meaning of the sound intensity polarization in far more simple sound field conditions than those encountered in the opera house, a preliminary set of measurements of this quantity has been performed inside a duct. The experimental set-up and the significant results of this test are reported in Appendix A. From these it can be realized that, given a structural geometry of the acoustic system, (a) when holding the frequency band fixed, the sound intensity polarization mostly depends on the termination, and (b) when holding the termination fixed, the dependence on frequency of the intensity polarization is mostly linked to the excited proper modes of vibration.

As shown below, these arguments will be useful in the discussion of the collected measures inside the theater which consisted in a 1/3 octave band analysis ranging from 200 to 1250 Hz. First of all, the comparison of the overall values of the quantities measured inside the opeara house, shown in Table 1, defines the gross characteritics of the sound energy transfer. In fact, the inequality $L_R > L_P > L_v > L_I$ (where L_P and L_v stand for sound pressure and air velocity levels) holds for every measured point, thus indicating that the flow of energy is mostly localized rather than transmitted to outer regions by the active intensity. This can also be interpreted in terms of wavefronts: starting from the sound source, these are incident on and are reflected from the boundaries, thus providing information about the geometry and the materials of the hall. When, after the transient, the contribution of all reflections is gathered at the measurement point, the impinging wavefronts produce a sound pressure and a particle velocity whose time histories are substantially different from those due to the direct sound only. This model of propagation explains the build-up of standing waves in the hall which, together with progressive waves, are responsible respectively for the oscillations and radiative transfer of energy in the sound field. Then, the bipartition of the

TABLE 1

Overall levels 200–1250 Hz *of the sound levels of radiating intensity* L_I, *of air particle velocity* L_v, *of sound pressure* L_p, *and of oscillating intensity* L_R; *data are expressed in dB*: *reference values are* 10^{-12} W/m^2 *for intensities*, 2×10^{-5} Pa *for sound pressure and* 5×10^{-8} m/s *for particle velocity*; *errors are* 0·2 dB *for* L_I, L_v *and* L_p *and* 0·3 dB *for* L_R

Meaasurement point	L_I	L_v	L_p	L_R
I° order: Box 7	79·5	81·6	83	85·5
Stalls: row 11 — Seat 7/8	81·4	83·9	85·9	87
I° order: Box 17	79·6	81·5	82·8	84·2

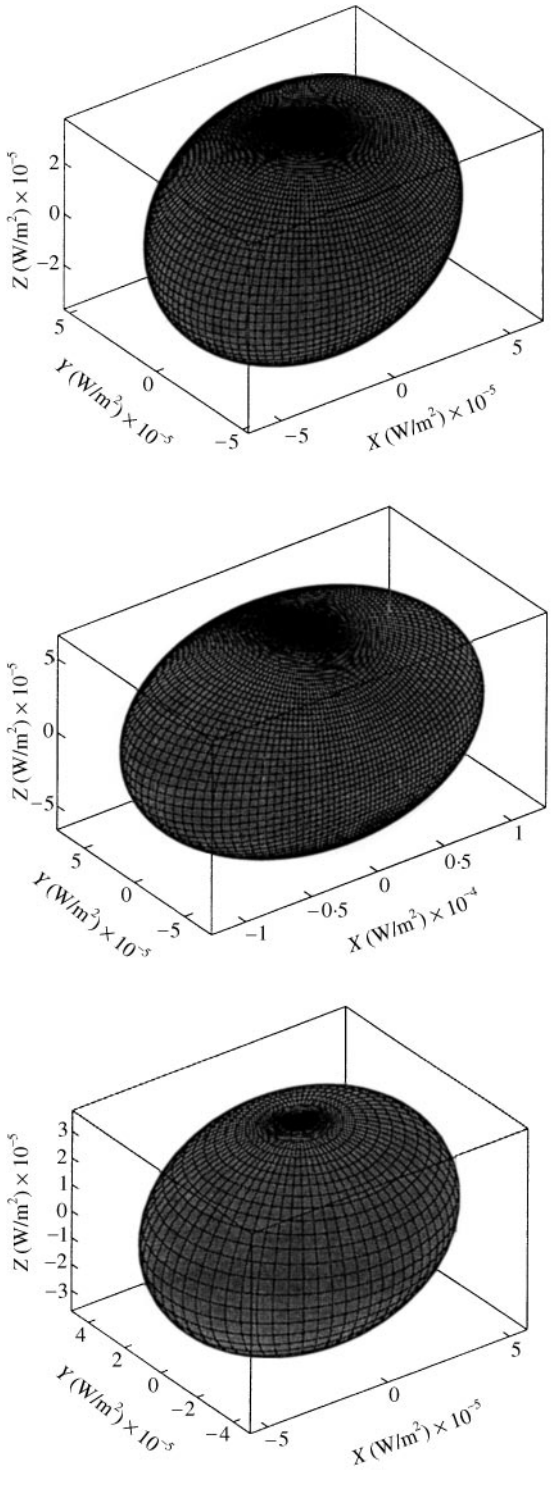

Figure 2. Ellipsoids of overall intensity polarization (200–1250 Hz) at three locations inside the opera house. From top to bottom: at the mouth of Box 7 of I° order, in the stalls at Row 11 between seats 7 and 8 (central position) and at the mouth of the symmetric Box 17 of I° order. The orientation of the reference frame is shown in Figure 1.

sound intensity is essentially due to the superposition of both fundamental kind of waves: standing and progressive.

Moreover, from Table 1 one realizes that, for the given measurement set-up (bare stage with orchestra shell present), the equality of the measured sound levels holds within experimental errors, so stressing a relation with the geometric symmetry of the hall. Only L_R seems to deviate a little, showing a wider gap between the two boxes.

In Figure 2 the geometrical aspects of the local storage of energy in the field are considered. The figure show the ellipsoids of the frequency overall sound intensity polarization respectively at the mouth of box 7, in the stalls and at box 17. It is evident that the central and lateral ellipsoids differ both in magnitude and in shape. The biggest ellipsoid measured in the stalls is obviously consistent with the highest level reported in Table 1. As regards the shape, all the three ellipsoids are stretched, but the stretching directions (the major axes of the ellipsoids) do not coincide. In the case of the central one, this direction is equal to the source–receiver line, while for the lateral ones it is slightly rotated; anyway, the major axis always belongs to the x–y plane of the measurement reference frame. Even though a complete investigation of the acoustic coupling of the box with the main space would require a complete intensity mapping of the mouth of the box, the slight rotation of the major axis of the sound intensity ellipsoids out of the source–receiver line is certainly due to the merging of the proper modes of the box with those of the main space for the fixed position of the source. In fact, the preliminary test inside the duct, had shown that the sound polarization is affected both by the absorbtions and the geometry of the acoustic system.

To spot further light on the way how oscillations of energy are distributed with frequency, Figure 3 shows the intensity polarization measured in the stalls for the 1/3 octave bands centered respectively at 1250, 630 and 315 Hz. What appears is a continuous deformation of the ellipsoids with lowering of frequency. In the highest band, the ellipsoid is squeezed along the z direction and gradually becomes stretched in the x direction. Moreover, some information is provided on how proper vibrations behave regarding the local oscillation of sound energy: they are isotropically distributed in the x–y plane at higher frequencies but are polarized along the source–receiver line at low frequencies.

Finally, Figure 4 shows the vector of overall radiating intensity at the location in the stalls. Here the direction of the vector is to the back of the hall pointing downwards. So, differently from oscillations of energy, which occur mainly on the x-axis in the front–back direction (see Figure 2) the net transfer of energy points to the place where the absorption is present, since the stalls are furnished with an array of upholstered seats.

3. THE COMPLETE ENERGETIC ANALYSIS OF THE TRANSIENT FIELD

As mentioned in the introduction, a complete energetic analysis of the transient sound field has been performed inside the theatre by means of the extension of the well-known statistical procedure introduced by Schroeder in the 1960s. The collected data are reported below and briefly discussed.

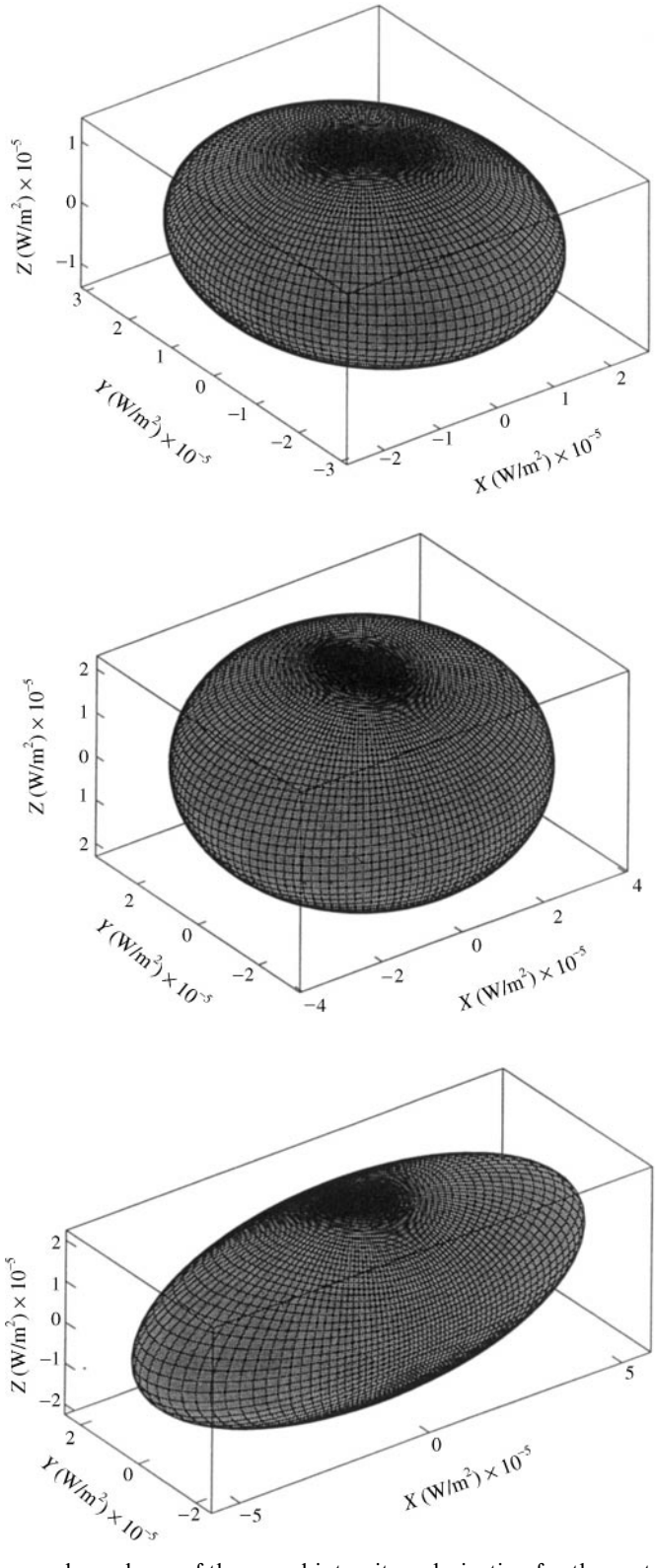

Figure 3. Frequency dependence of the sound intensity polarization for the central position in the stalls (see Figure 1). From top to bottom: 1/3 oct. band centred respectively at 1250, 630 and 315 Hz.

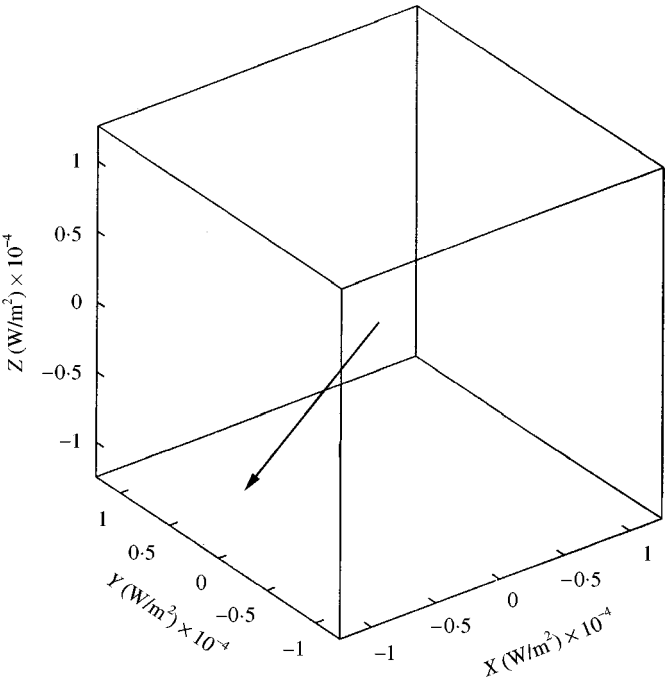

Figure 4. The vector of the overall active intensity (200–1250 Hz) at the central position in the stalls. Note that the direction is different from the major axis of the relative ellipsoid of polarization shown in Figure 2. The arrow points downwards where the sound absorbing furniture is present.

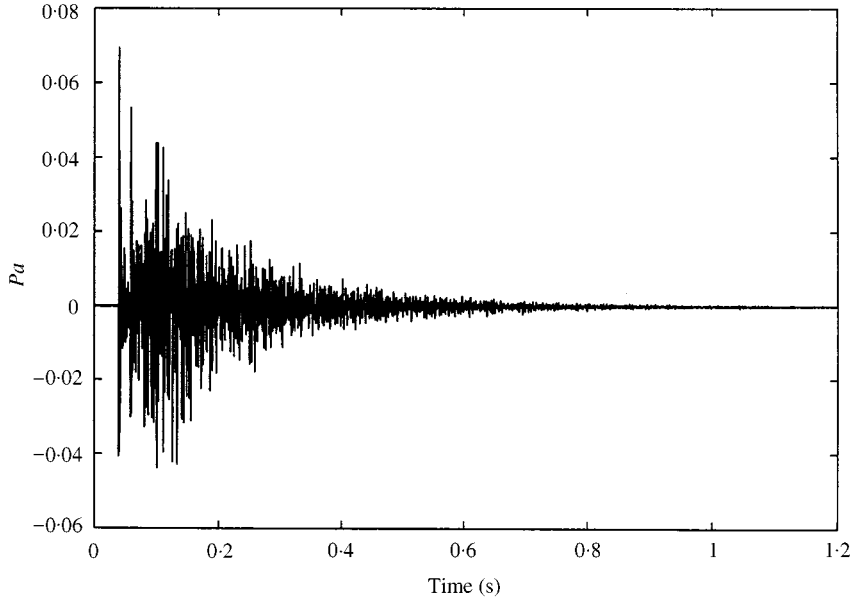

Figure 5. Pressure impulse response at the central stall. The frequency range is the same as that of the steady state measurment (200–1250 Hz).

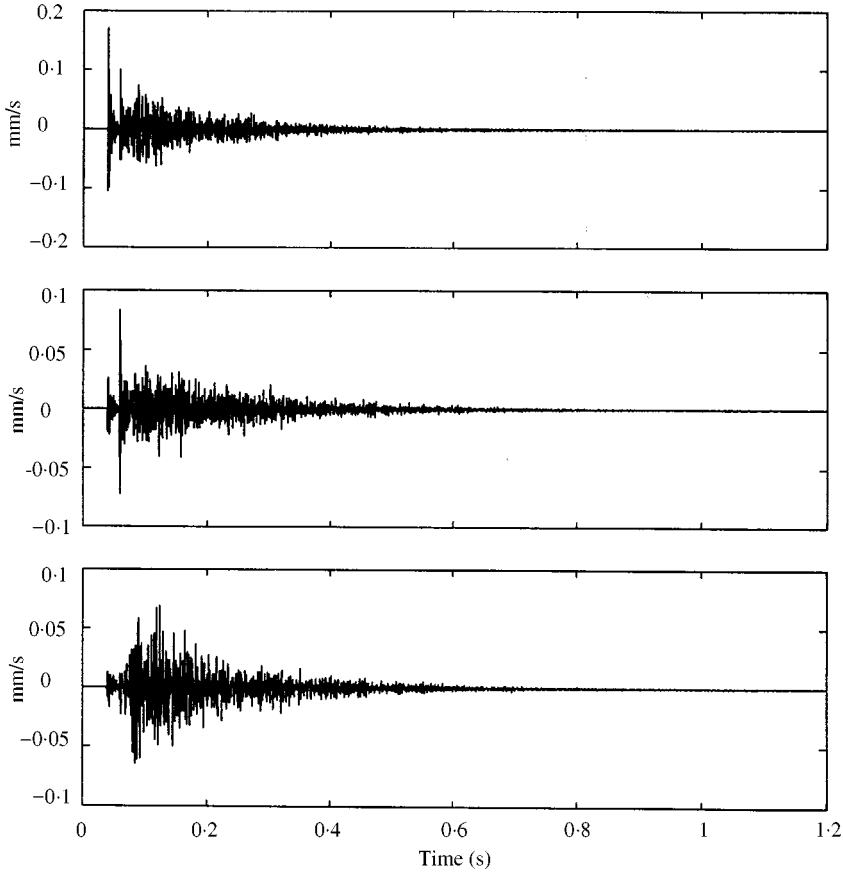

Figure 6. Air particle velocity impulse response at the central stall. From top to bottom: x, y, z, components.

In Figures 5 and 6 the impulse responses of the sound pressure and of the three components of the air particle velocity are visualized for the position in the stalls. While the plot of Figure 5 is obtained by means of a standard one-channel MLS program, the three components of the air velocity impulse responses are obtained implementing the procedure detailed in Appendix B. The transient pressure gradient has been calculated by the usual finite difference approximation, starting from three pairs of close pressure signals acquired along every orthogonal spatial direction. As is evident, the implemented algorithm is sufficiently precise to give the possibility of appreciating the different transient behaviours of the three velocity components.

The transient behavior of the three components of sound intensity at the central position in the stalls is shown in Figure 7. Here it is interesting to note that the transient along the y-axis shows an almost symmetric oscillation about the zero line, differently from the other two directions, characterized by a predominantly negative energy flow. These results give a precise energetic image of the acoustical environment as seen from the measuring point (see Figure 1): in fact, the x component

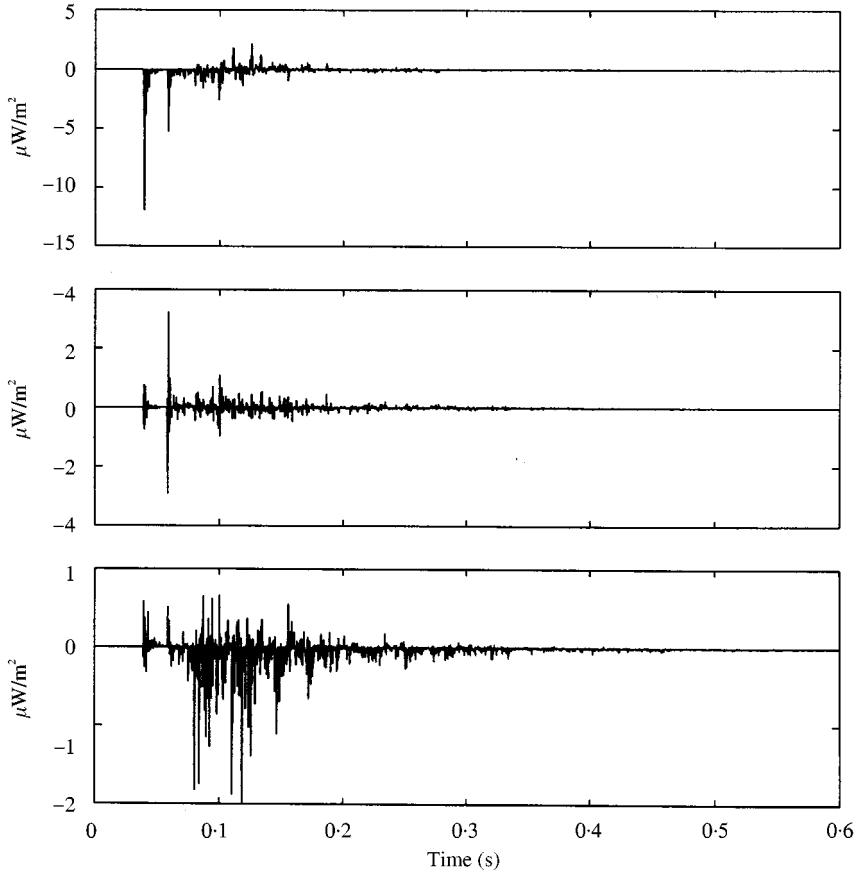

Figure 7. Transient time history of the sound intensity at the central stall. From top to bottom: x, y, z, components.

reveals that the sound energy is mainly coming from the stage even during the transient, while the behavior of the z component is due to the combined effects of reflections from the ceiling and the absorptions of the stalls. On the other hand, the y component takes account of the concomitant reflections from the lateral walls.

Figure 8 shows the total sound energy decay obtained from Eq. (7) in the central position of the stalls (the decays at the other two mesurement points are quite similar). Dfferently from the general case discussed in reference [8], no relevant differences in the decays of the kinetic and potential parts have been found. The decay does not perfectly follow the simple exponential law foreseen for diffused fields; nonetheless, an estimate of the reverberation time (T_{60}) can be given by a straight-line fitting of the decay curve over the first 30 dB: the result is about 1·4 s.

Figures 9 and 10 respectively show the sound intensity decays registered at the stalls position and at the mouth of box no. 7.

Figure 9 is derived from the transient time histories displayed in Figure 7. The above noted oscillating nature of the y transient makes its statistical average almost

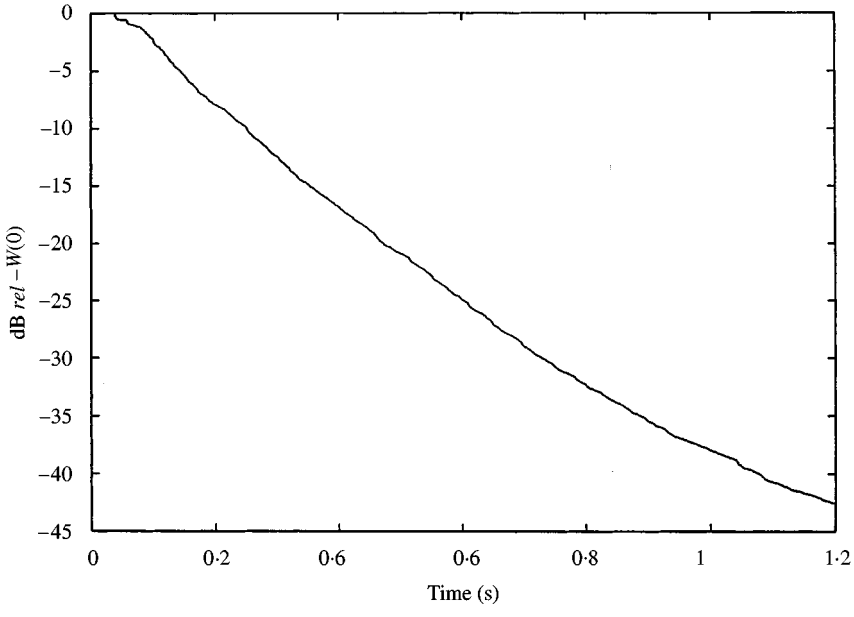

Figure 8. Decay of total sound energy at the central stall (log scale)

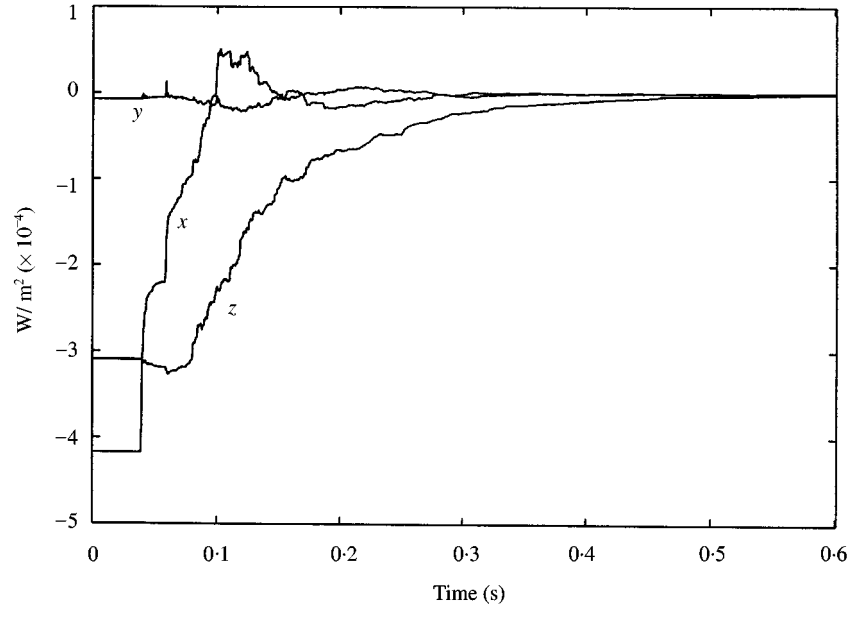

Figure 9. Single components of sound intensity decay at the central stall.

null during all the decay: this happens in particular at the initial instant ($t = 0$), where due to the ergodicity of the acoustic system the statistical average coincides with the ordinary stationary time average. As regards the x and the z decays, it can be observed that they start from negative values so confirming the discussion

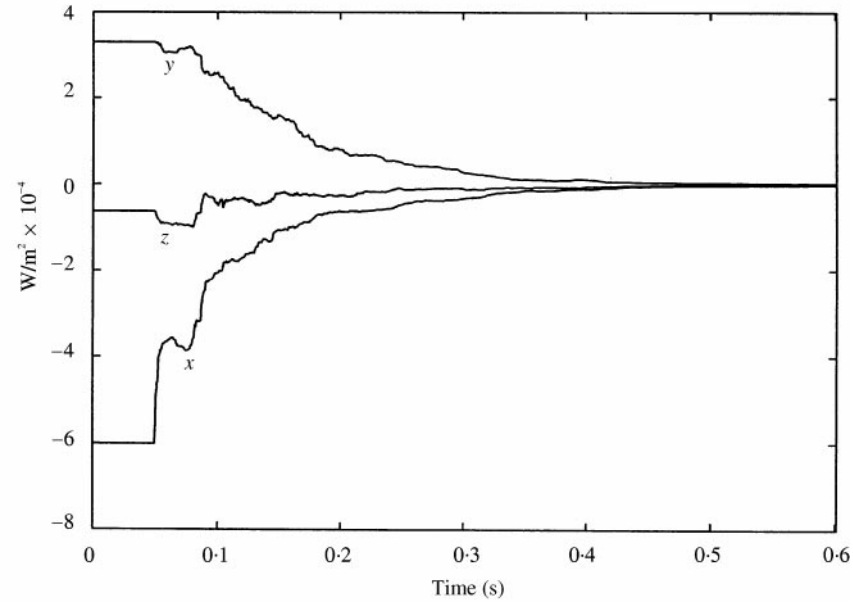

Figure 10. Single components of sound intensity decay at Box 7.

already done for the corresponding transient time histories. Moreover, upon looking at the x decay, it can be noted that its representative curve is not a monotonic one, given that it algebraically accounts for the relative signs of the impulse responses of sound pressure and air velocity

Differently from Figure 9, Figure 10 shows that now, the intensity along z is negligible: this happens due to the vertical confinement of the sound field at the mouth of the box. Furthermore, the negative value of the x component, together with the positive ones of y, confirms the presence of a strong direct flow of sound energy from the source towards the inside of the box enclosure.

Finally, the values of T_{60}, σ and η defined in section 1·3 were collected. While the first two quantities are practically independent of the position ($T_{60} \cong 1{\cdot}4$ s and $\sigma \cong 0{\cdot}98$) the values of η (about 0·3 at the stalls position and 0·4 at the mouths of both the boxes) are not. This means that the sound energy is homogeneously well balanced between its kinetic and potential parts, but the sound field tends to be more radiative at the mouths of the two boxes.

4. CONCLUSIONS

A full energetic analysis of the sound field generated under standard testing conditions inside an Italian opera house, has been accomplished during the steady and transient states, following an original approach developed in recent years. The measured quantities were: the sound intensity polarization, the total sound energy density and the intensity decays, together with two energetic field indicators called

σ and η. Three locations were investigated: the mouths of two first order opposite boxes and the central stalls between them.

As discussed in sections 2 and 3, the overall energetic analysis of the experimental data reveals the predominant contribution of direct sound both for energy oscillations (steady state measurements) and radiative phenomena (transient measurements) at all the three locations. In particular, it was found that the largest fraction of energy flow is oscillating-like and that the set of modes excited by the source used stored sound energy mainly along the source receiver line. However, a more detailed analysis shows that the polarization direction is affected by the frequency band as shown in Figure 3. The very similar data obtained at the boxes acoustically confirm the architectural symmetry of the hall.

The combined rigorous analysis of the transient energy flows together with the total energy decays has shown that at different measurement positions the sound decay can happen in a very different way from the energy flux point of view but in a quite similar way when looking at the energy. This fact is confirmed also by the substantial invariance of the reverberation time T_{60} with respect to the different values found for the energy transfer indicator η in the different positions.

Finally, it can be concluded that the results obtained by this new rigorous approach confirm the potentiality of all the new defined quantities for the physical interpretation of energetic phenomena involved in architectural acoustics.

REFERENCES

1. G. Schiffrer and D. Stanzial 1994 *Journal of the Acoustical Society of America* **96**, 3645–3653. Energetic properties of acoustic fields.
2. D. Stanzial, N. Prodi and G. Schiffrer 1996 *Journal of the Acoustical Society of America* **99**, 1868–1876. Reactive acoustic intensity for general fields and energy polarization.
3. D. Stanzial and N. Prodi 1997 *Journal of the Acoustical Society of America* **102**, 2033–2039. Measurements of newly defined intensimetric quantities and their physical interpretation.
4. F. J. Fahy 1987 *Sound Intensity*. London: Elsevier.
5. M. R. Schroeder 1965 *Journal of the Acoustical Society of America* **37**, 409–412. New methods for measuring reverberation time.
6. D. Bonsi 1998 *Ph. D. Dissertation, University of Ferrara, Ferrara, Italy*. Theoretical and experimental study of energetic properties of confined sound fields.
7. P. M. Morse and K. U. Ingard 1986 *Theoretical Acoustics*. Princeton, NJ: Princeton University Press.
8. D. Stanzial and D. Bonsi 1998 *Proceedings of International Symposium on Musical Acoustics, Leavenworth, WA, USA*, 365–370. Towards a local theory of reverberation: monitoring the behavior of the energetic quantities during the sound decay within a duct.

APPENDIX A: SOUND INTENSITY POLARIZATION INSIDE A DUCT

Figure A1 shows the set-up employed for the test measurements of sound intensity polarization inside a duct.

The sound field was generated within a plexiglass duct, with a square section of 28×28 cm and 4 m long, by an MLS system and a loudspeaker. The duct, having

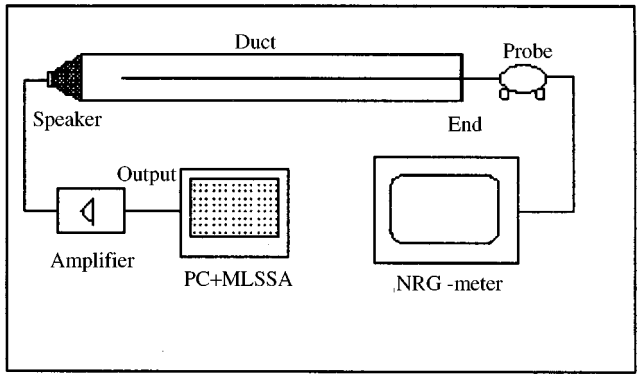

Figure A1. Experimental set-up for testing measurements in a duct. NRG-meter is the virtual instrument specifically developed for measuring the newly defined intensimetric quantities.

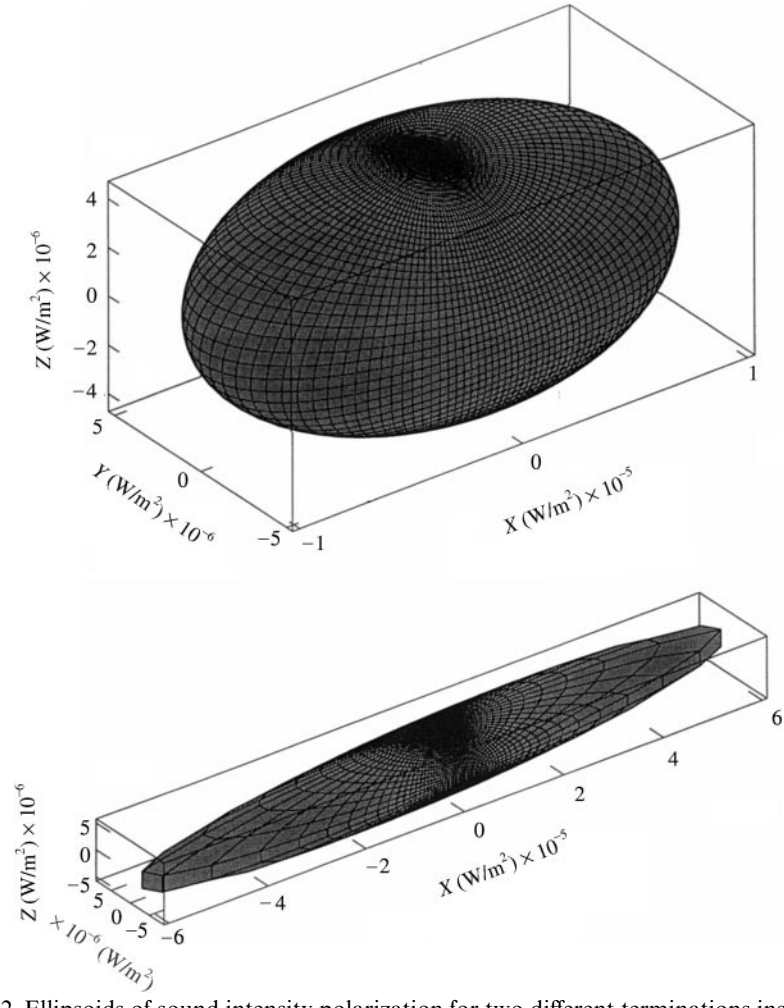

Figure A2. Ellipsoids of sound intensity polarization for two different terminations inside the duct of Figure A1. The plots refer to the 1/3 oct. band centered at 1 kHz which is above the cut-off frequency of the duct (614 Hz). The measurement position is at 1 m from the termination. Top: foam rubber termination; bottom: aluminum termination.

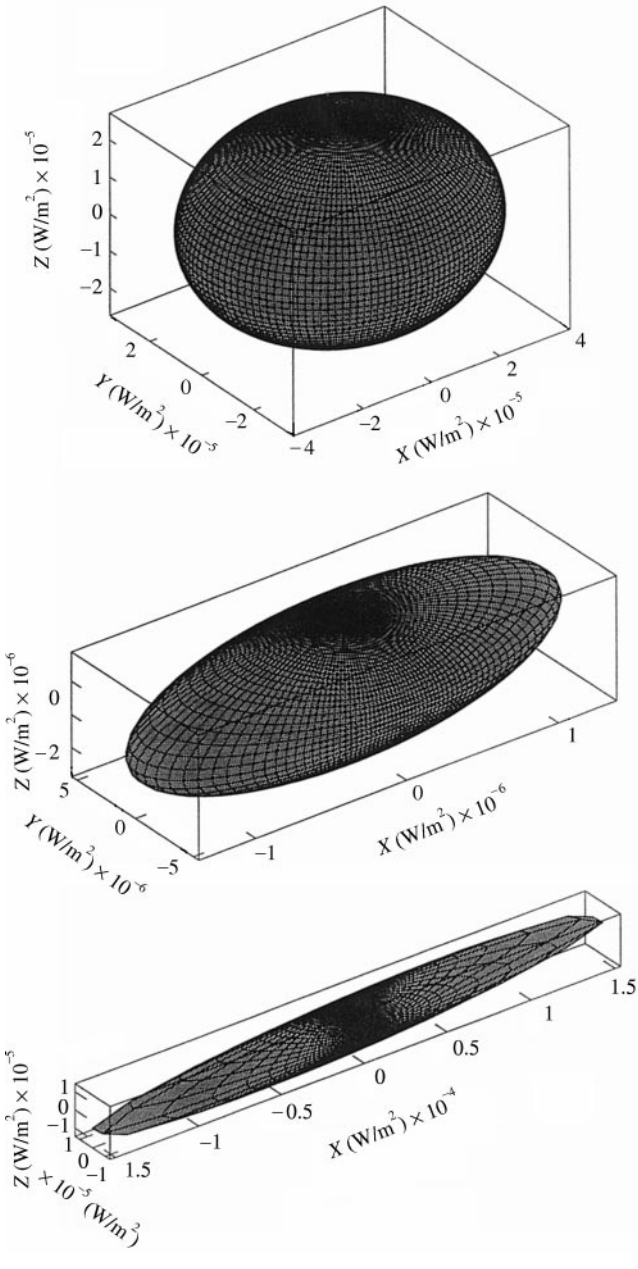

Figure A3. Frequency dependence of the sound intensity polarization with the foam rubber termination inside the duct. From top to bottom: 1/3 oct. band centered respectively at 2500, 800 and 200 Hz.

a cut-off frequency at about 614 Hz, was terminated with two very different kinds of absorbing boundaries: a foam rubber layer and an aluminum panel. A 3-D intensity probe was used to collect simultaneously the sound pressure signals from six close positions inside the duct and processed by a purpose-built sound intensity meter.

Figures A2 and A3 show the results obtained. In the former the sound intensity polarization levels and the full ellipsoids are reported when changing the aborptions (a), (b) but keeping the geometry of the acoustic system unchanged. In the latter the effect of changing the geometry of the acoustic system with the same absorption conditions is monitored by means of a proper filtering procedure above and below the duct cut-off frequency.

APPENDIX B: IMPULSE RESPONSE OF AIR PARTICLE VELOCITY

We now present a brief derivation of the result used in the main test regarding the air particle velocity impulse response: a more complete treatment of this subject can be found in reference [6]. Any linear acoustic field is completely defined by a scalar function: the kinetic potential $\phi(\mathbf{x}, t)$. The usual sound pressure is expressed by the relation

$$p(\mathbf{x}, t) = -\rho_0 \, \partial\phi(\mathbf{x}, t)/\partial t. \tag{B1}$$

If the sound source has a point-like extension and its temporal behavior is given by the function $s(t)$, the quantity $\phi(\mathbf{x}, t)$ may be written as a *time convolution*

$$\phi(\mathbf{x}, t) = \int_{-\infty}^{t} \mathrm{d}\tau \, g(\mathbf{x}, t - \tau) s(\tau), \tag{B2}$$

where $g(\mathbf{x}, t)$ represents the *potential impulse response*, satisfying the wave equation

$$\Delta g(\mathbf{x}, t) - \frac{\mathbf{1}}{c^2} \frac{\partial^2 g(\mathbf{x}, t)}{\partial t^2} = \delta(\mathbf{x})\delta(t)$$

and the appropriate boundary conditions imposed by the environment. According to equations (B1) and (B2), it can be shown that

$$p(\mathbf{x}, t) = \int_{-\infty}^{t} \mathrm{d}\tau \, g(\mathbf{x}, t - \tau) s_p(\tau), \tag{B3}$$

where $s_p(t) = -\rho_0 \partial s(t)/\partial t$ turns out to be the pressure excitation.

The air particle velocity may be found by means of the Euler equation

$$\mathbf{v}(\mathbf{x}, t) = -\frac{1}{\rho_0} \int_{-\infty}^{t} \mathrm{d}\tau \, \nabla_p(\mathbf{x}, \tau).$$

It follows that

$$\mathbf{v}(\mathbf{x}, t) = \int_{-\infty}^{t} \mathrm{d}\tau \left(-\frac{1}{\rho_0} \int_{0}^{t-\tau} \mathrm{d}t' \, \nabla g(\mathbf{x}, t') \right) s_p(\tau).$$

Therefore, upon defining the function

$$\mathbf{g}_v(\mathbf{x}, t) = -\frac{1}{\rho_0}\int_0^t \mathrm{d}\tau\, \nabla g(\mathbf{x}, \tau)$$

it is possible to express the particle velocity $\mathbf{v}$ through a convolution between $\mathbf{g}_v$ and the same excitation s_p of the sound pressure relation (equation (B3)). In practice

$$\mathbf{v}(\mathbf{x}, t) = \int_{-\infty}^{t} \mathrm{d}\tau \mathbf{g}_v(\mathbf{x}, t - \tau) s_p(\tau),$$

which states that $\mathbf{g}_v$ is just the air velocity impulse response.